Available online at www.sciencedirect.com
SCIENCE DIRECT®
Journal of Catalysis 242 (2006) 58–70
JOURNAL OF CATALYSIS
www.elsevier.com/locate/jcat

CO oxidation on partially oxidized Pd nanoparticles

T. Schalow, B. Brandt, M. Laurin, S. Schauermann, J. Libuda [*,1], H.-J. Freund

Fritz-Haber-Institut der Max-Planck-Gesellschaft, Faradayweg 4-6, 14195 Berlin, Germany

Received 13 April 2006; revised 23 May 2006; accepted 23 May 2006

Available online 30 June 2006

Abstract

Combining multi-molecular beam (MB) experiments and in situ time-resolved infrared reflection absorption spectroscopy (TR-IRAS), we studied the relationship between the formation of Pd surface oxides and the reaction kinetics of CO oxidation on a well-defined Fe_3O_4-supported Pd model catalyst. The model catalyst was prepared in-situ under ultra-high-vacuum (UHV) conditions by Pd deposition onto a well-ordered Fe_3O_4 film on Pt(111). In previous studies, structure, morphology, and adsorption properties of the model system, as well as the formation of Pd oxide species, were characterized in detail. At low reaction temperatures ($T < 450$ K), the CO oxidation activity of partially oxidized Pd particles was found to be significantly lower than that of metallic Pd particles. We address this deactivation of the catalyst to a weak CO adsorption on Pd surface oxides, leading to a very low reaction probability. Even after extended exposure to CO-rich reactants at 400 K, no significant gain in catalytic activity due to reduction of surface oxides was observed. As a result, we conclude that the formation of Pd oxide species at higher temperatures causes long-term deactivation of the catalyst at lower temperatures. At higher reaction temperatures ($T \geqslant 500$ K), however, Pd oxides can be dynamically formed and decomposed, depending on the composition of the reactant environment. Although Pd oxides are formed on the surface under O-rich conditions, such oxide species are decomposed under CO-rich conditions at these temperatures. Using a simple model, we qualitatively analyzed the formation and decomposition process of Pd oxides under reaction conditions. We found that at higher reaction temperatures, partial oxidation of the Pd particles generally led to reduced CO oxidation activity and slow hysteresis effects that were strongly dependent on the pretreatment of the sample.

Keywords: Model catalysts; Surface reaction kinetics; Molecular beams; Surface oxidation; Palladium; Iron oxide; CO oxidation

1. Introduction

Oxide-supported metal nanoparticles are commonly used as catalysts for oxidation reactions in chemical industry, emission control, and energy technology [1,2]. In many cases, it is assumed that the activity and selectivity of the catalysts sensitively depends not only on the size and morphology of the active metal particles, but also on the chemical nature of the oxygen species. Depending on oxygen pressure and temperature various oxygen species (i.e., chemisorbed oxygen, subsurface oxygen, surface oxides and bulk metal oxides) have been observed even on simple single-crystal surfaces of transition metals [3–17]. It has been reported that the formation of such oxides is connected to strong changes in the catalytic activity [18–20]. However, in most cases the role of the various oxygen species in the kinetics of oxidation reactions is not well understood. The situation is more intricate for oxide-supported metal particles considering the simultaneous presence of different facets; edge, corner, and defect sites; modified lattice and electronic structures; and specific particle–support interactions. All of these effects may critically control the formation of the different oxygen species and thereby strongly influence catalytic activity and selectivity.

To correlate the catalytic activity with the formation of different oxygen species and oxides, we combined well-defined model catalyst surfaces, molecular beam (MB) methods, and time-resolved infrared reflection absorption spectroscopy (TR-IRAS). The use of model catalysts is motivated by the vast structural complexity of real heterogeneous catalysts and their limited accessibility to surface science techniques. Supported model catalysts, in contrast, provide clean, well-defined sur-

* Corresponding author.
E-mail address: joerg.libuda@chemie.uni-erlangen.de (J. Libuda).
[1] New address: Lehrstuhl für Physikalische Chemie II, Universität Erlangen-Nürnberg, Egerlandstr. 3, D-91058 Erlangen, Germany.

0021-9517/$ – see front matter
doi:10.1016/j.jcat.2006.05.021

faces with strongly reduced complexity that can be easily characterized at the atomic level (see e.g. [21–25] for recent reviews on model catalysts). The activity of these model surfaces is probed by multi-MB experiments under well-defined reaction conditions. Simultaneously, the catalyst surface is characterized by in situ TR-IRAS. This approach allows us to obtain information on CO and oxide surface coverage under reaction conditions.

Recently, we studied the formation of different oxygen species on a Pd/Fe_3O_4 model catalyst over a broad range of temperatures [26–28]. For oxidation temperatures up to 450 K, oxygen primarily chemisorbs dissociatively on metallic Pd surface areas; however, at temperatures of 500 K and above, Pd oxide species also form. Oxide formation occurs initially at the particle–support interface and, at a later stage, also on the outer particle surface. In this study, we focus on the role of these different oxygen species in CO oxidation kinetics. It is shown that the activity of the model catalyst for CO oxidation decreases drastically with increasing coverage of the Pd surface by oxides. For reaction temperatures below 450 K, partial oxidation of the Pd surface, obtained by oxygen exposure at higher temperatures, results in a long-term deactivation of the catalyst, because the decomposition of such surface oxides is kinetically hindered. However, at temperatures above 450 K, Pd oxide species can be formed under O-rich conditions and decompose under CO-rich conditions. As a result, the average oxidation state and the activity of the catalyst change dynamically depending on the composition of the reactant environment. Nonetheless, the CO_2 formation rate of partially oxidized Pd particles is generally significantly reduced compared with that of metallic Pd particles.

2. Experimental

All MB and IRAS experiments were performed in a UHV apparatus at the Fritz-Haber Institut (Berlin), as described previously [29]. The system offers the experimental possibility of crossing up to three beams on the sample surface. A schematic representation of the setup is shown in Fig. 1a. Both effusive beams were generated by doubly differentially pumped sources based on multichannel arrays and modulated using remote-controlled shutters. The beam intensities were adjusted in fully computer-controlled sequences in the range of 1.1×10^{13} to 2.2×10^{14} molecules $cm^{-2}\,s^{-1}$. Both sources were operated at room temperature. The beam diameters were chosen such that they exceeded the sample diameter. All experiments were performed using high-purity O_2 (Linde, 99.999%) and CO (Linde, 99.997%, further purified by a gas filter [Mykrolis]). An au-

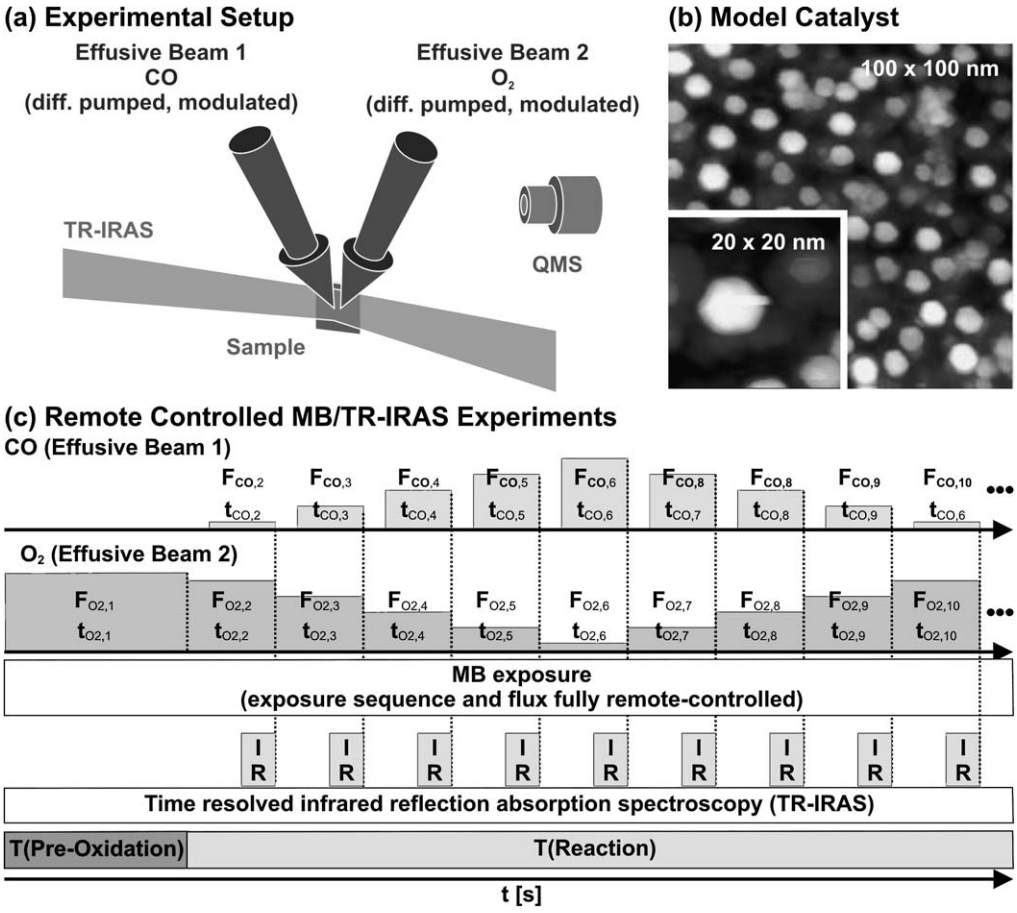

Fig. 1. (a) Schematic representation of the molecular beam setup and (b) STM image of the supported Pd model catalyst (STM of Pd/Fe_3O_4 by Starr and Shaikhutdinov [27]). (c) Illustration of the of experimental sequence of the fully automated molecular beam CO oxidation experiments: exposure, TR-IRAS and temperature sequence.

tomated quadrupole mass spectrometer (QMS) system (ABB Extrel) was used for gas-phase detection. All QMS data were corrected with respect to blind experiments using an catalytically inert sample surface [Fe_3O_4/Pt(111)]. IR spectra were acquired by a vacuum FTIR spectrometer (Bruker IFS 66v/s) with a spectral resolution of 2 cm^{-1} (using an MIR polarizer to select the p-component of the IR light only).

The thin (∼100 Å) Fe_3O_4 film was grown on Pt(111) by repeated cycles of Fe (>99.99%, Goodfellow) deposition and subsequent oxidation (see [30,31] for details). Cleanliness and quality of the oxide film was checked by IRAS of adsorbed CO and LEED. Pd particles (>99.9%, Goodfellow) were grown by physical vapor deposition (Pd coverage 2.7×10^{15} atoms cm^{-2}; sample temperature 115 K) using a commercial evaporator (Focus, EFM 3, flux calibrated by a quartz microbalance). Directly after Pd deposition, the sample was annealed at 600 K and stabilized by 5 cycles of oxygen (8×10^{-7} mbar for 1000 s) and CO exposure (8×10^{-7} mbar for 3000 s) at 500 K. An STM image of the model surface is shown in Fig. 1b.

3. Results and discussion

3.1. Experimental setup and model system

The experimental approach applied in this study to correlate kinetic data and structural information of supported Pd model catalysts under well-defined reaction conditions is briefly summarized in Fig. 1. As a model catalyst, we used Pd particles deposited by physical vapor deposition (PVD) on a thin, well-defined Fe_3O_4 film grown on Pt(111). The Pd particles and Fe_3O_4 film were prepared in situ under UHV conditions. Before the experiments, the sample was repeatedly oxidized and reduced to obtain a stable surface under the experimental conditions applied in this study [27]. Growth, structure, and adsorption properties of the Pd particles and the Fe_3O_4 support were recently studied in detail [27,32]. Most importantly, the crystalline Pd particles grow uniformly on the support (island density 8.3×10^{11} islands cm^{-2}), covering about 20% of the catalyst surface. The particles consist of ∼3000 atoms and have an average diameter of ∼7 nm. They expose mainly (111) facets (∼80%), but also a smaller fraction of (100) facets (∼20%). A scanning tunneling microscopy (STM) image of the model catalyst is shown in Fig. 1b.

To connect the catalytic activity of the model catalyst on CO oxidation to the surface structure of the Pd particles under reaction conditions, various remote-controlled MB/TR-IRAS experiments were performed. In these experiments, all parameters—temporal modulation of MB exposure (pulse duration, $t_{O_2,i}$, $t_{CO,i}$), O_2 and CO MB flux ($F_{O_2,i}$, $F_{CO,i}$), surface temperature (T), and acquisition of IR spectra (IR)—were performed in a fully computer-controlled sequence and could be individually adjusted (see Fig. 1c). This procedure allowed us to systematically study the kinetics in an extremely reproducible fashion and over a broad range of parameters. To scrutinize the influence of Pd oxide formation on the kinetics of CO oxidation, the model catalyst was first oxidized at a defined temperature, leading to partial oxidation of the Pd particles. Subsequently, the sample was cooled in oxygen to the reaction temperature. This procedure is referred to as "preoxidation" in what follows. In the next step, the reaction kinetics of the model catalyst were probed for various O_2/CO ratios by using pulses of O_2 and CO of variable intensity (typically, the total pressure of CO and O_2 was kept constant). At each O_2/CO ratio, the sample was first exposed to an O_2 beam only, before the CO beam was switched on and the CO_2 formation rate was recorded. After a reaction time of about 360 s, the system approached steady-state conditions, and the steady-state CO_2 formation rate could be determined from the QMS signal. (Note that the exact time depends on surface temperature and stoichiometry of the reactants.) In addition, IRAS spectra were recorded using CO as a probe molecule, allowing us to characterize the state of the surface under reaction conditions. Finally, the CO beam was switched off again, and the flux of both MBs was readjusted for the next data point. In general, the experimental sequence was run from oxygen-rich conditions (i.e., high O_2 and low CO flux) to CO-rich conditions (i.e., low O_2 and high CO flux) and subsequently back to oxygen-rich conditions. Note that the total time scale of the complete experimental sequence was about 6 h, emphasizing the need to fully automatize this type of experiment.

The complete flux, temperature, and reaction rate data of a representative experiment are shown in Fig. 2a. Here the sample was first preoxidized at 500 K (8×10^{-7} mbar for 1000 s: 600 L [1 L of oxygen corresponds to 3.6×10^{14} molecules cm^{-2}]) to partially oxidize the Pd particles and was subsequently cooled in oxygen to the reaction temperature of 450 K. In the next step, the reaction kinetics were systematically probed as function of the CO/O_2 ratio. We characterize this ratio by defining the fraction of CO x_{CO} in the total flux of CO and O_2 as

$$x_{CO} = F_{CO}/(F_{CO} + F_{O_2}),$$

with F_{CO} and F_{O_2} representing the fluxes of CO and O_2, respectively.

We started under oxygen-rich conditions ($x_{CO} = 0.05$) by adjusting the oxygen and CO flux to the desired composition of the reactant atmosphere at a constant total pressure of 8×10^{-7} mbar. Subsequently, the reactant composition was stepwise varied to $x_{CO} = 0.95$ (CO-rich conditions) and back to $x_{CO} = 0.05$. At each data point, the model catalyst was first exposed to oxygen, and subsequently, the second reactant (CO) was admitted while the transient and steady-state CO formation kinetics were recorded. In addition, IR spectra were taken at most data points under steady-state conditions (as shown in Fig. 2a); a total of 31 IR spectra were acquired during the full sequence.

The raw QMS data of the above-described experiment are shown in Fig. 2b. Note that CO and oxygen were recorded on $m/z = 29$ ($^{13}C^{16}O$) and $m/z = 34$ ($^{18}O^{16}O$), respectively, for intensity reasons. As shown in the lower two graphs in Fig. 2b, the intensity of both reactant beams, CO and O_2, followed the pulse sequence indicated in Fig. 2a. The upper graph of Fig. 2b depicts the CO_2 formation rate during the entire experiment. The CO_2 formation rate under steady-state conditions for each stoichiometric data point can be derived from the CO_2 signal at

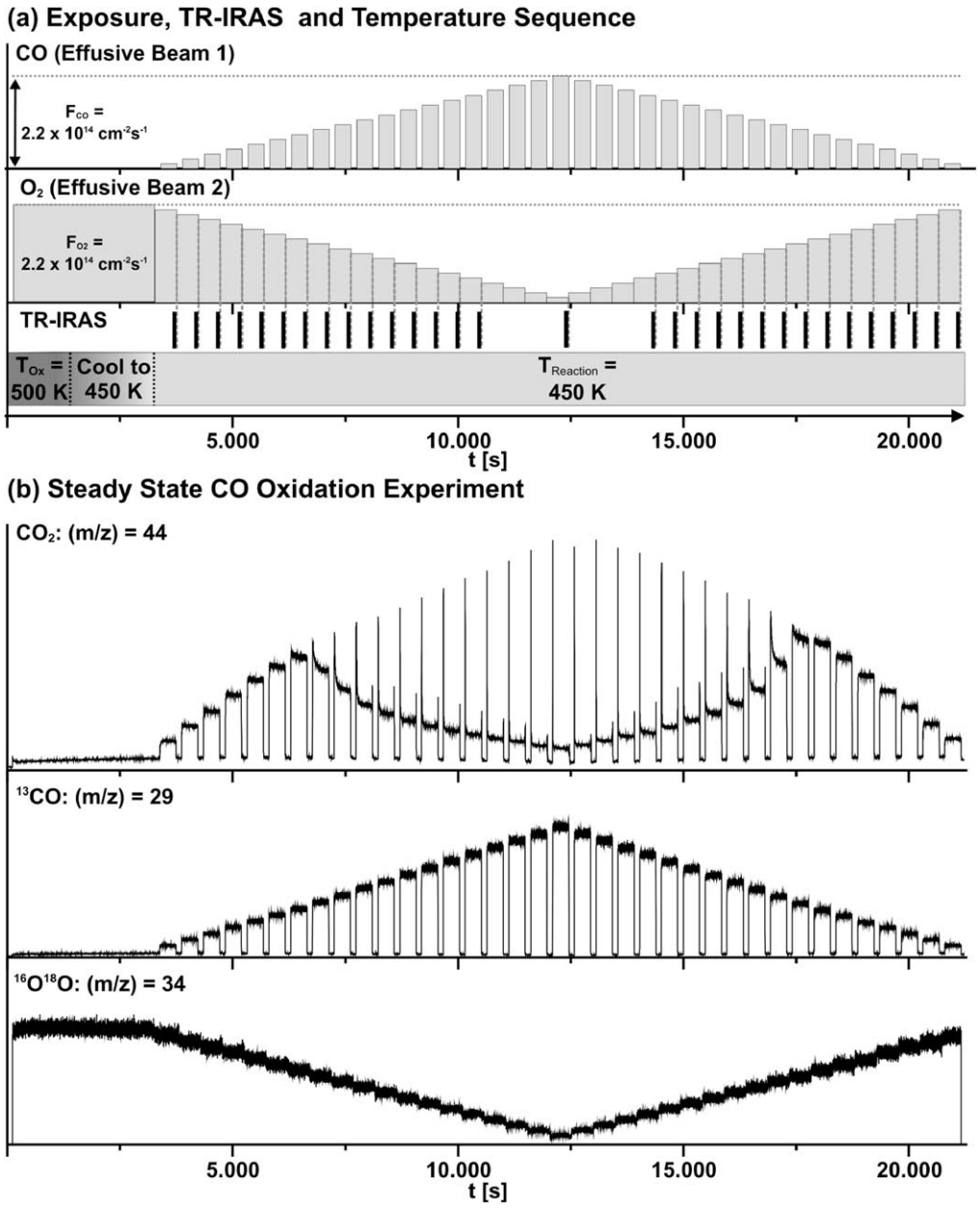

Fig. 2. (a) Exposure, TR-IRAS and temperature sequence of an automated MB CO oxidation experiment at 450 K after preoxidation at 500 K: First the sample is exposed to oxygen at 500 K (8×10^{-7} mbar, 1000 s: 600 L) and cooled in oxygen to 450 K. Subsequently, the CO oxidation kinetics were probed as function of the CO and O_2 flux (at a total constant effective pressure of 8×10^{-7} mbar). (b) Raw QMS signal of CO_2 ($m/z = 44$), CO ($m/z = 29$) and O_2 ($m/z = 34$) during the experiment.

the end of each CO pulse after the system has reached steady-state conditions. A more detailed discussion on the transient behavior of the CO_2 formation has been provided elsewhere [33,34].

3.2. CO oxidation kinetics versus reaction temperature

In a first step, we investigated the CO_2 formation rate as a function of CO/O_2 ratio at different surface temperatures (400–500 K). The exposure and temperature sequence of the corresponding experiments is depicted in Fig. 3a. First, the sample was exposed to oxygen (120 s) to establish a fully oxygen-precovered surface. Subsequently, CO was switched on to start the reaction. After a reaction time of about 360 s (with the exact time depending on the surface temperature and stoichiometry of the reactants), the system reached steady-state conditions, and the CO_2 formation rate was determined from the QMS signal. In addition, IRAS spectra were acquired. The experiments were started under oxygen-rich reaction conditions ($x_{CO} = 0.05$), and the stoichiometry was then gradually shifted in steps of 0.05 toward CO-rich conditions ($x_{CO} = 0.95$).

Fig. 3b shows the steady-state CO_2 formation rate as a function of x_{CO} for different surface temperatures. It is seen that under oxygen-rich conditions (low x_{CO}), CO_2 formation increased linearly with CO partial pressure. Surprisingly, at 500 K, CO_2 production was significantly lower for low x_{CO} than that at

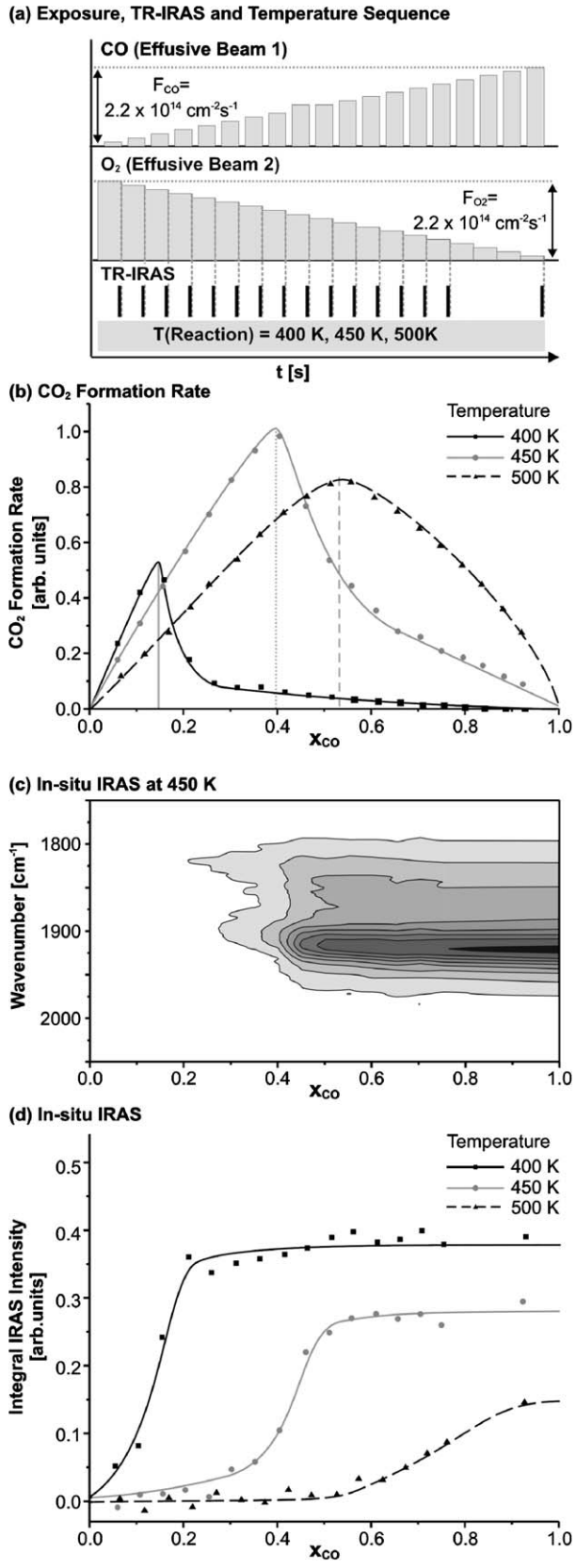

Fig. 3. CO oxidation on a Pd/Fe_3O_4 model catalyst for different reaction temperatures: (a) exposure, TR-IRAS and temperature sequence of the experiments; (b) steady state CO_2 formation rate, (c) in situ IRAS spectra and (d) IRAS: integral intensity in the CO stretching frequency region as a function of CO and O_2 flux (total effective pressure: 8×10^{-7} mbar).

400 K. With increasing x_{CO}, at a certain value the CO_2 production began to decrease rapidly. Two points are important here. First, the transition point was reached at a significantly lower CO mole fraction, x_{CO}, at 400 K ($x_{CO,Trans} \sim 0.15$) than at 500 K ($x_{CO,Trans} \sim 0.55$). Second, the decreased CO_2 formation rate at the transition point was more pronounced at lower reaction temperatures. As a result, the CO_2 formation rate increased with increasing temperature under CO-rich conditions, whereas it decreased with increasing temperature under O-rich conditions.

Additional information on the state of the surface can be obtained from the in situ IR spectra, depicted in Fig. 3c ($T = 450$ K). Under oxygen rich conditions ($x_{CO} < 0.2$), almost no features could be observed in the CO stretching frequency region. At the transition point, however, two features typical for CO adsorption at a stretching frequency of 1850 and 1920 cm^{-1} appeared and rapidly gained intensity with increasing x_{CO}, indicating a rapid buildup of CO coverage. For $x_{CO} > 0.6$, the intensity of the IR features became nearly independent of x_{CO}. The integral IRAS intensity of both features is shown in Fig. 3d; qualitatively, the behavior was similar for all reaction temperatures; although under oxygen-rich conditions almost no CO adsorption was found, the signal rapidly increased around the transition point until it finally was saturated under CO-rich conditions. (Note that the IRAS intensities may not yield accurate quantitative information on the surface coverage as a result of dipole coupling effects; see [35] for details.)

CO oxidation on Pd surfaces has been extensively discussed in recent theoretical and experimental studies [33,34,36,37]. Briefly, two reaction regimes, O-rich and CO-rich, have been identified. In the first regime, under oxygen-rich conditions, the reaction rate is controlled by CO adsorption. The CO sticking coefficient is expected to decrease only slightly with increasing temperature due to a reduced lifetime of the CO precursor state. However, on γ-Al_2O_3 supported Pd particles, this effect is too weak to notably affect the reaction rate [34]. Consequently, the reaction rate is anticipated to scale linearly with the CO partial pressure independently of the surface temperature. In the second regime, under CO-rich conditions, the reaction rate is controlled by dissociative oxygen adsorption. This step is significantly inhibited by CO adsorption (referred to as CO poisoning in what follows), being the cause of the low reaction rate under CO-rich conditions [38]. Under steady-state conditions, CO coverage critically depends on the sticking coefficient, CO desorption, and CO consumption by the reaction. Although the first of these processes is largely temperature-independent, the latter two are faster at higher surface temperatures. Consequently, the CO coverage is lower and the associated poisoning effect is weaker at higher temperatures, resulting in a higher reactivity. Both reaction regimes are interconnected by the transition region, in which a rapid increase of CO coverage is associated with a drop in the CO_2 formation rate. With increasing surface temperature, the transition point shifts toward higher x_{CO} due to faster CO desorption and consumption.

In view of the above discussion, the results of this study are generally in good agreement with the results of previous work [36]. However, one point in the present study stands in

sharp contrast to previous experiments: The reaction rate was found to decrease rapidly with increasing surface temperature under O-rich conditions. For example, no correlation between temperature and reaction rate was observed in previous work on Al_2O_3-supported Pd particles at high O_2 and low CO flux [34,36]. The explanation for the lack of temperature dependence is simple: The rate-determining step for CO oxidation under O-rich conditions is CO adsorption. The CO total adsorption probability over the temperature range depends on the sticking coefficient on the Pd particles and an additional contribution due to the so-called "capture zone effect" (i.e., trapping on the support and diffusion to the particles, see, e.g. [21,25] for detailed discussions). Both effects would be expected to show only weak temperature dependence over the temperature interval studied.

For the Pd/Fe_3O_4 model catalyst, under the conditions applied in this study, there is one fundamental difference from the previous experiments on Pd/Al_2O_3: We recently showed that on the Pd/Fe_3O_4 model catalyst, large amounts of Pd oxide species can be formed on oxygen exposure at 500 K [26,39]. These Pd oxide species are initially formed at the particle–support interface, but later also on the remaining particle surface. With increasing oxidation temperature, the fraction of the Pd surface that becomes oxidized increases. Therefore, we suggest that the lower CO_2 formation rate at higher temperatures under O-rich conditions is due to partial oxidation of the Pd particles.

Oxidation can affect the CO oxidation rate via two possible mechanisms. The first of these results from the low activity of the Pd oxide phase itself. As discussed recently, the PdO phases formed show much lower reaction probabilities toward CO compared with metallic O-precovered Pd (cf. [26,28]). The second mechanism may be due to the capture zone, the efficiency of which is expected to sensitively depend on the properties of the support and the particle–support interface. This effect may be reduced due to PdO formation at the particle–support interface. It may be speculated that oxidation of the particle–support interface can result in decreasing flux of CO to the Pd particles.

3.3. CO oxidation kinetics versus oxide formation at low temperatures

In view of the experiments discussed in the previous section, we have suggested that the formation of Pd oxide species lowers the activity of the model catalyst at 500 K under O-rich conditions. To study the influence of Pd oxide formation on the reaction kinetics of CO oxidation under steady-state conditions in more detail, we performed combined MB/TR-IRAS steady-state experiments on preoxidized Pd particles.

The exposure and temperature sequence of the experiments is schematically represented in Fig. 4a. First, the sample was preoxidized (8×10^{-7} mbar for 1000 s: 600 L) at different oxidation temperatures (450–600 K), leading to partial oxidation of the particle surface. Subsequently, the sample was cooled to the reaction temperature (400 or 450 K) in oxygen. Finally, the reaction kinetics on the model catalyst was studied as a function of CO/O_2 ratio. For each CO/O_2 ratio, the sample was first exposed to oxygen only (formation of an oxygen-saturated surface) and then to both reactants at a given x_{CO}. After steady-state conditions were established, the CO_2 formation rate was determined by QMS and IRAS spectra acquired under reaction conditions.

The left column of Fig. 4 shows the CO_2 formation rate (b) and integral intensity in the CO stretching frequency region of the IRAS spectrum (c) as functions of stoichiometry for a reaction temperature of 400 K. Along with the preoxidized samples, a non-preoxidized (i.e., fully reduced) sample was also subjected to MB/TR-IRAS steady-state experiments as a reference. The qualitative behavior of the CO_2 formation rate was relatively similar independent of the preoxidation temperature; in any case, under O-rich conditions, the reaction rate scaled almost linearly with the CO partial pressure. At the transition point between the O-rich and the CO-rich region at $x_{CO} \sim 0.15$, the CO_2 formation rate dropped sharply, resulting in a very low reaction rate under CO-rich conditions. A detailed discussion of the steady-state behavior has been given previously [25,34]. Quantitatively, however, the CO_2 formation rate on the preoxidized samples decreased drastically with increasing preoxidation temperature. After preoxidation at 550 K, the reaction rate was ∼65% lower with respect to the reduced sample.

The IRAS intensity in the CO stretching frequency region as a function of CO/O_2 ratio is shown in Fig. 4c. In all cases, CO coverage increased under O-rich conditions up to $x_{CO} \sim 0.2$, whereas for $x_{CO} > 0.2$, almost constant CO coverage occurred on further increases in CO partial pressure. Again, it should be noted that IRAS intensities do not directly reflect the CO coverage due to dipole coupling effects [35]. However, it was apparent that the total CO coverage decreased with increasing preoxidation. Preoxidation at 550 K resulted in a ∼60% lower IRAS intensity of adsorbed CO. The decrease in CO signal with increasing degree of oxidation can be related to the weak adsorption of CO on oxidized Pd (cf. [28]).

The CO_2 formation rate (d) and the integral absorption of adsorbed CO in IRAS (e) for a reaction temperature of 450 K are shown in the right column of Fig. 4. Briefly, a similar behavior was observed as for 400 K; the CO_2 formation rate increased linearly with the CO flux under O-rich conditions until it drops at the transition point, which now is near $x_{CO} \sim 0.4$. As at a reaction temperature of 400 K, a substantially decreased CO_2 formation rate with increasing preoxidation temperatures was observed at 450 K (Fig. 4d). This is in accordance with the reduced intensity of adsorbed CO in IRAS on the preoxidized samples, indicating a lower CO coverage under steady-state conditions (Fig. 4e).

The IRAS data obtained under reaction conditions directly reflect the oxidation behavior of the Pd/Fe_3O_4 model catalyst, as was studied recently [26–28]. It was found that with rising oxidation temperature, an increasing fraction of the Pd particle surface was covered by surface oxides. Although the Pd surface remained mainly metallic for oxidation temperatures up to 450 K, metallic Pd surface areas and surface oxides coexisted on the particles in the temperature range of 500–550 K. However, the formation of such Pd surface oxides significantly modified the adsorption properties of the model catalyst, dras-

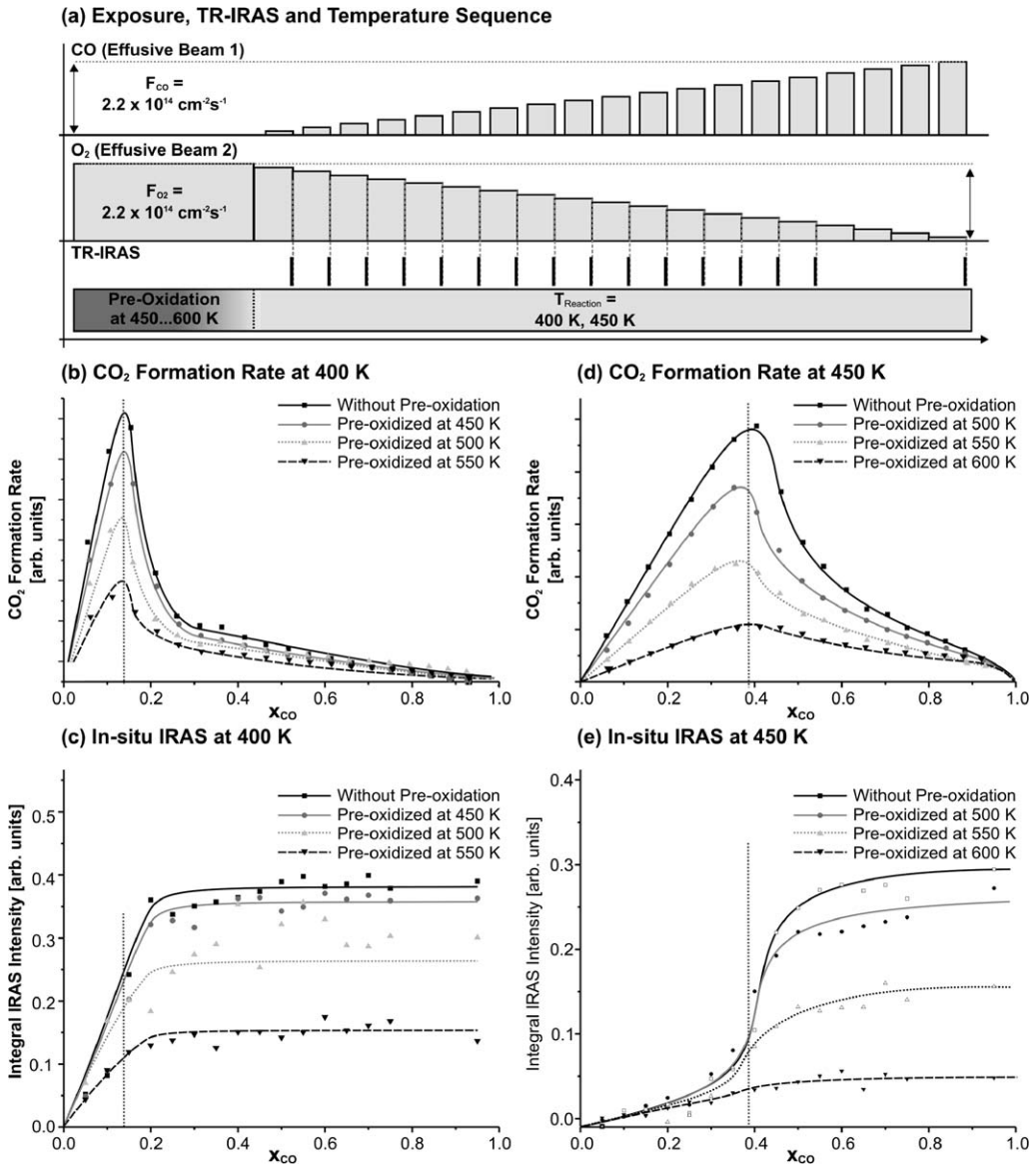

Fig. 4. CO oxidation on partially oxidized Pd/Fe_3O_4 model catalysts at low reaction temperatures: (a) exposure, TR-IRAS and temperature sequence of the experiments; (b), (d) steady state CO_2 formation rate and (c), (e) IRAS: integral intensity in the CO stretching frequency region as a function of the CO and O_2 flux at a surface temperature of 400 and 450 K, respectively.

tically lowering its CO and oxygen adsorption capacity. Even at low temperatures ($T = 115$ K), no CO adsorption on Pd surface oxides was observed under the conditions applied in this study ($p_{CO} \sim 10^{-6}$ mbar).

In view of these results, two main conclusions can be drawn from the experiments shown in Fig. 4. The most important of these is the reduced CO_2 formation rate with increasing preoxidation temperature for both reaction temperatures. It is apparent that the lower catalytic activity of the preoxidized samples was related to the formation of surface oxides. The IRAS results show that essentially no CO adsorption occurred on the oxidized Pd phases. Hence, CO oxidation likely occurred mainly on metallic Pd surface areas involving chemisorbed oxygen. This conclusion is in line with recent CO titration experiments indicating negligible activity of Pd surface oxides for CO oxidation [26].

Second, it is noteworthy that the reaction rate was lower on the preoxidized system than on the nonoxidized sample even under CO-rich conditions, where dissociative oxygen adsorption was the rate-limiting step of the reaction. Here an additional oxygen supply by decomposition of Pd oxides enhancing the CO_2 formation on the catalyst surface could be invoked. However, even after extended exposure to the reactants at 400 K under CO-rich conditions, no significant increase of the CO coverage could be observed in IRAS, which would indicate a reduction of the Pd surface on the preoxidized sample (see Fig. 4c). Therefore, we presume that the reduction of Pd oxide species by CO was kinetically hindered at low reaction temperatures. As a consequence, the formation of Pd surface oxide species at higher reaction temperatures caused a long-term deactivation ($>10^4$ s) of the catalyst at lower reaction temperatures.

3.4. CO oxidation kinetics versus oxide formation at high temperatures

Earlier in this paper, we noted that the formation of Pd surface oxides is connected to deactivation of the model catalyst for all CO/O_2 ratios at low reaction temperatures. Apparently, strong kinetic hindrances, which inhibit decomposition of the Pd oxide phases at lower temperatures, lead to preserved deactivation even under reducing conditions. At 500 K, however, we have recently shown that Pd surface and interface oxides may slowly decompose, providing additional oxygen for CO oxidation [26]. To gain more detailed insight into the formation and decomposition of Pd oxide species and their kinetic implications under reaction conditions, we also performed MB/TR-IRAS experiments at higher reaction temperatures.

First, the sample was oxidized at 550 K (8×10^{-7} mbar for 1000 s: 600 L) and then cooled to the reaction temperature (500 K). A reference experiment without preoxidation was also performed. Next, the reaction kinetics of the model catalyst was probed systematically over a broad range of CO/O_2 ratios by varying the intensity of the reactant beams. The experimental sequence was started under O-rich conditions (i.e., $x_{CO} \sim 0$), and the fraction of CO in the reactant atmosphere was stepwise increased to $x_{CO} \sim 1$, that is, CO-rich conditions (denoted by first run). Subsequently the sequence was inverted from $x_{CO} \sim 1$ to 0 (denoted by second run) (see Fig. 5a). For each CO/O_2 ratio, the sample was first saturated by oxygen (O_2 beam only, 120 s) and then simultaneously exposed to a CO and O_2 beam of appropriate intensity. After a reaction time of 360 s, the CO_2 formation rate was determined by QMS, and IRAS spectra were acquired under reaction conditions.

The CO_2 formation rate (b, c) and IRAS spectra (d) of the preoxidized sample are shown in the left column of Fig. 5. While switching from O-rich to CO-rich (first run) and CO-rich to O-rich (second run) conditions, a qualitatively similar behavior of the reaction rate is observed, as discussed earlier. The CO_2 formation rate increased steadily with the CO flux under O-rich conditions ($x_{CO} < 0.5$) and with the O_2 flux under CO-rich conditions ($x_{CO} > 0.65$) (see Fig. 5b). But comparing the absolute CO_2 formation rate of the first and second runs reveals pronounced differences; the reaction rate of the second run was significantly higher than that of the first run throughout the entire experiment.

To analyze the differences between the first and second runs, the relative activity of the catalyst (which we define as the CO_2 formation rate of the second run normalized with respect to the rate of the first run) is calculated in Fig. 5c. Because the activity is closely related to the degree of oxidation of the Pd surface, the quantity may also be interpreted as the relative degree of surface oxidation in the second run relative to the first run. Note that the second run was performed by switching from CO-rich (high x_{CO}) to O-rich (low x_{CO}) conditions. In the CO-rich regime ($x_{CO} > 0.65$), the relative activity of the catalyst was found to increase steadily with increasing time of sample exposure to the CO-rich reactants, that is, with decreasing x_{CO}. Finally, at the transition point, the CO_2 formation rate of the second run was enhanced by ~1.8 with respect to the first run. This behavior indicates substantial surface reduction during the reaction under CO-rich conditions.

Switching to the O-rich regime ($x_{CO} < 0.5$), the relative activity first decreased with increasing exposure to the reactants (i.e., decreasing x_{CO}) and finally settled at a CO_2 formation rate of about 1.4 times higher during the second run for $x_{CO} < 0.2$. This behavior indicates that the surface was partially reoxidized under O-rich conditions.

The O-rich and CO-rich regimes also can be identified by IRAS of adsorbed CO (see Fig. 5d). Under O-rich conditions, no significant CO adsorption could be observed, whereas the CO coverage increased steadily with increasing CO flux under CO-rich conditions. However, CO coverage on the sample was significantly higher during the second run compared with the first run in the CO-rich regime, also indicating a reduction of surface PdO under reaction conditions.

When discussing the CO oxidation experiments at 500 K, it is important to take into account the fact that Pd oxide species can be formed on oxygen exposure and can decompose on CO exposure under the present conditions. We assume that formation or decomposition of Pd oxide is controlled by the CO/O_2 ratio or, more precisely, by whether the reaction is performed in the CO-rich or the O-rich regime.

Under O-rich conditions ($x_{CO} < 0.5$), the CO_2 formation rate increased steadily with CO partial pressure. This fits qualitatively well with our previous results. However, the absolute CO_2 formation rate in the first run under O-rich conditions was relatively low compared with that for the nonpreoxidized sample and the second run of the preoxidized sample. Taking into account that after oxidation at 550 K, a major fraction of the particle is covered by Pd surface oxides [27,28], the low activity under O-rich conditions can be attributed to the high surface oxide coverage. The CO_2 formation rate increased linearly with the CO flux in this regime, indicating a nearly constant degree of surface oxidation.

Switching to CO-rich conditions ($x_{CO} > 0.65$), an increasing CO coverage on the metallic Pd surface with increasing CO flux was observed in the IRAS spectra (see Fig. 5d). The CO_2 formation rate decreased with an increasing CO/O_2 ratio in this regime. Interestingly, the reaction rate (Fig. 5b) and CO adsorbate coverage (Fig. 5d) were significantly enhanced during the second run compared with the first run. In addition, the slope of the CO_2 formation rate during the first run became substantially steeper with increasing x_{CO}. Both findings indicate that the activity of the catalyst increased in the CO-rich regime.

To evaluate the changes in the activity of the model catalyst under reaction conditions in more detail, we calculated the relative activity of the catalyst, that is, the CO_2 formation rate of the second run normalized on the first run (see Fig. 5c). In the CO-rich regime, the relative activity of the catalyst increased with decreasing x_{CO}, that is, increasing reaction time under CO-rich conditions. The CO_2 formation rate at the transition point was nearly twice as high for the second run than for the first run. We assign the higher reaction rate during the second run to a partial reduction of the preoxidized Pd surface and an increasing fraction of metallic Pd surface area available

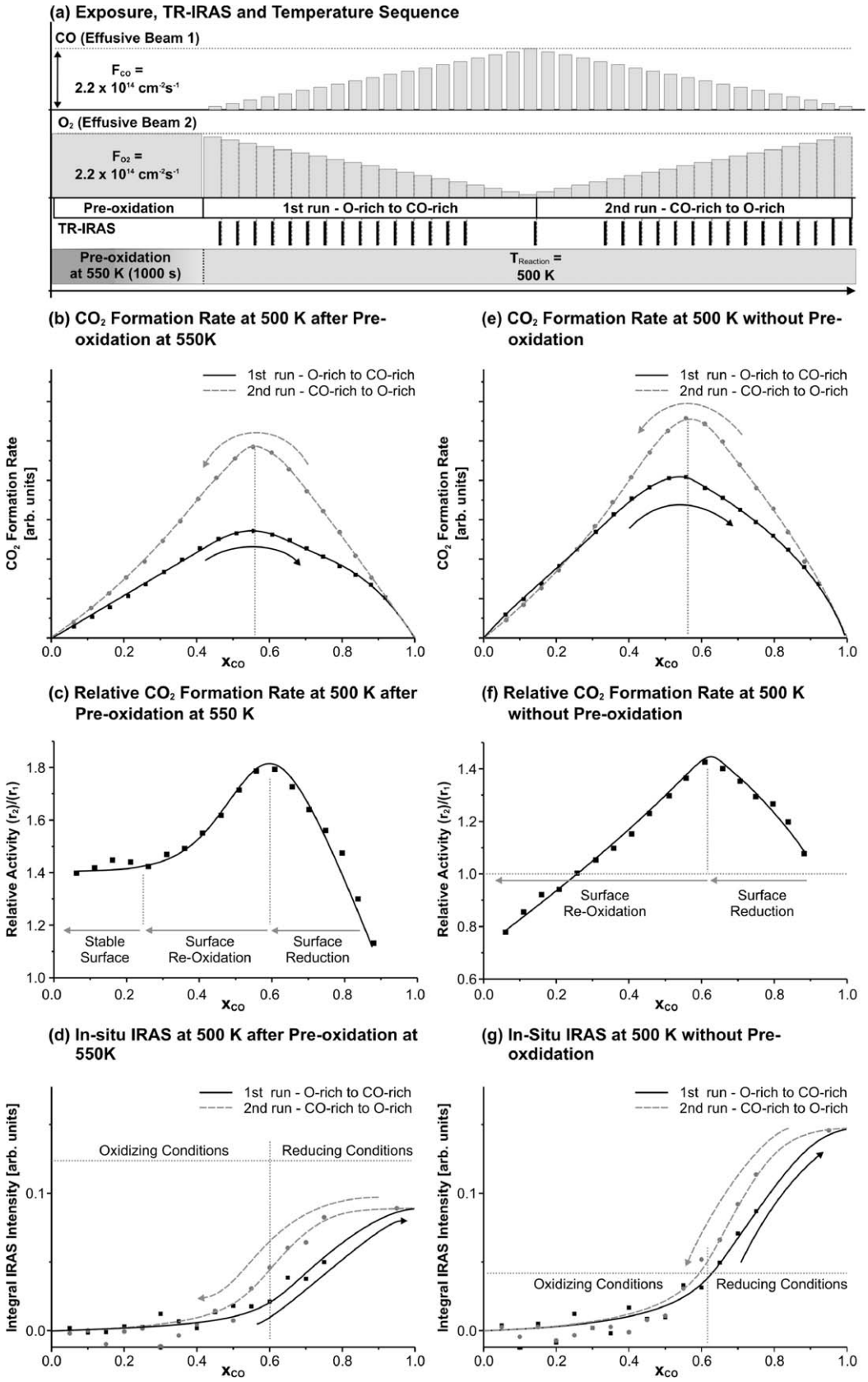

Fig. 5. CO oxidation on Pd/Fe_3O_4 model catalysts at 500 K under conditions of dynamic oxidation and reduction: (a) exposure, TR-IRAS and temperature sequence of the experiments; (b), (e) quasi steady state CO_2 formation rate, (c), (f) relative CO oxidation activity during 2nd run (increasing O_2 flux, decreasing CO flux) relative to the 1st run (decreasing O_2 flux, increasing CO flux) and (d), (g) IRAS: integral intensity in the CO stretching frequency region as a function of the CO and O_2 flux after preoxidation at 550 K and on the reduced model catalyst.

for CO oxidation. Considering that the Pd surface was mainly CO-covered in this regime, it is reasonable to assume a reduction of Pd surface oxides by CO under these conditions. This assumption is further corroborated by IRAS spectra showing increased CO adsorption on the model catalyst during the second run. It was recently shown that the formation of Pd surface oxides drastically lowered the catalyst's CO adsorption capacity [27,28]. Consequently, partial reduction of the catalyst is associated with increased CO adsorption.

Switching back to the O-rich regime ($x_{CO} < 0.5$), in the second run, the CO_2 formation rate was still enhanced compared with the first run (see Fig. 5b). However, this enhancement decreased with increasing reaction time under O-rich conditions (see Fig. 5c). Finally, for $x_{CO} < 0.2$, no further changes in the activity of the catalyst could be observed on proceeding exposure to the O-rich conditions and the CO_2 formation rate to be ∼1.4 higher than at the beginning of the experiment. Two important points are noteworthy here. First, the relative activity of the catalyst decreased under O-rich conditions. Under these conditions, the Pd surface was mainly oxygen-covered, and no CO adsorption was detected by IRAS (see Fig. 5d). From the linear slope of the CO_2 formation with increasing CO partial pressure in this regime during the first run, we can conclude that the degree of oxidation was nearly constant. However, during the second run, the CO_2 formation rate did not scale linearly with respect to the CO partial pressure, indicating modification of the catalyst surface. Hence, we attribute the decreased relative activity to reoxidation of the surface during the second run. Reoxidation of the metallic Pd surface occurred mainly between $x_{CO} \sim 0.5$ and 0.2 and finally became very slow. Second, it is important to point out that the activity of the catalyst during the second run was ∼1.4 times higher for low x_{CO} than during the first run. Obviously, oxidation at 500 K did not yield the same oxide coverage as the preoxidation at 550 K. This finding is in good agreement with a recent IRAS experiment showing that with rising oxidation temperature, an increasing fraction of the Pd surface became oxidized [27,28].

For the non-preoxidized sample, a qualitatively similar behavior was observed, as depicted in the right column of Fig. 5. Again, it is found that the CO_2 formation rate increased steadily with the CO flux under O-rich conditions ($x_{CO} < 0.5$) and with the O_2 flux under CO-rich conditions ($x_{CO} > 0.65$) (see Fig. 5e). However, the reaction rate on the non-preoxidized sample was significantly higher than on the preoxidized sample throughout the entire experiment. The relative activity of the model catalyst during the second run with respect to the first run is shown in Fig. 5f. In the CO-rich regime ($x_{CO} > 0.65$), the activity increased steadily with increasing reaction time under CO-rich conditions, until a ∼1.4-times higher activity occurred at the transition point ($x_{CO} \sim 0.55$). In the O-rich regime, however, decreasing catalyst activity with increased exposure to the O-rich reactants was observed. Finally, a lower CO_2 formation rate during the second run was observed for $x_{CO} < 0.2$. The enhanced CO_2 formation rate in the CO-rich regime of the second run was also reflected by in situ IRAS (Fig. 5g); here, the CO coverage was higher during the second run than during the first run. Again, it should be noted that the CO coverage on the non-preoxidized sample considerably exceeded the coverage on the preoxidized sample.

According to the foregoing, the behavior of the CO_2 formation rate on the non-preoxidized sample can be explained as follows. At the beginning of the experiments (low x_{CO}, first run), the surface of the Pd particles was mostly in a metallic reduced state, with high activity for CO oxidation. With increasing exposure to the O-rich environment, the Pd surface became partially oxidized, reflected by the steep slope of the CO_2 formation rate at the beginning, which decreased slightly on extended exposure. However, the reaction rate still remained significantly higher compared with that for the preoxidized sample. Therefore, we suggest that only a relatively small fraction of the particle surface became covered by Pd oxides. In fact, recent IRAS experiments [28] and the reactivity studies at low reaction temperatures (see above) also showed that at 500 K, only a relatively small fraction (∼35%) of the Pd surface was oxidized, whereas oxidation at 550 K and above resulted in a largely oxidized surface.

Switching from O-rich to CO-rich conditions, the behavior was comparable to that of the preoxidized sample; the reaction rate during the second (decreasing x_{CO}) run was substantially enhanced compared with the first run (increasing x_{CO}). Fig. 5f shows the relative activity change between the two runs (i.e., the CO_2 formation rate of the second run divided by the rate during the first run) as a function of x_{CO}. Similar to the preoxidized sample, the relative activity increased with increasing reaction time in the CO-rich regime, that is, with decreasing x_{CO}. At the transition point between the CO-rich and O-rich regimes, the CO_2 formation rate was ∼1.4 times higher in the second run than in the first run (compared with the ∼1.8-times higher activity found for the preoxidized sample; see above).

Again, we link the higher CO_2 formation rate during the second run in the CO-rich regime to the larger metallic Pd surface area available on the particles as a result of partial reduction of the surface oxide by adsorbed CO. Because of the relatively small initial surface oxide coverage after oxidation at 500 K, the gain in activity due to partial surface reduction for the non-preoxidized sample was smaller than for the sample preoxidized at 550 K. Additional evidence for this assumption is provided by the in situ IRAS spectra shown in Fig. 5g; the CO coverage under "quasi-steady-state" conditions on the non-preoxidized surface was substantially higher than after preoxidation at 550 K, indicating a lower coverage of surface oxides ("quasi-steady-state," because the formation and decomposition of Pd oxides is a dynamic process, which, however, is much slower than equilibration of the coverage of chemisorbed CO and O with the gas phase). It is also noteworthy that the hysteresis of the CO coverage observed by IRAS, reflecting the partial reduction of the Pd surface, is more pronounced for the preoxidized sample.

When switching to the O-rich regime, the relative activity of the model catalyst was steadily decreased with increasing reaction time under O-rich conditions. Interestingly, the CO_2 formation rate during the second run (decreasing x_{CO}) was smaller than during the first run (increasing x_{CO}) for very low x_{CO} values ($x_{CO} < 0.2$). Apparently, the degree of Pd surface oxidation

after extended reaction under O-rich conditions exceeded the amount of surface oxide formed during preoxidation at the beginning of the experiment.

In summary, the results of the CO oxidation experiments at 500 K show that, in contrast to the low-temperature experiments, the average oxidation state of the catalyst surface is dynamically modified under reaction conditions depending on the composition of the reactant environment. The surface oxide formation and reduction behavior are closely coupled to the two reaction regimes of CO oxidation. Whereas under O-rich conditions, the Pd surface oxide coverage constantly increases, slow reduction of Pd surface oxides occurs in the CO-rich regime. The most important conclusion concerning catalytic behavior is that formation/decomposition of the surface oxides directly controls the activity of the model catalyst for CO oxidation. The rate of CO_2 formation decreases with increasing surface oxide coverage, indicating low activity of the surface oxides. Finally, it should be pointed out that maximum oxide coverage degree and the kinetics of surface oxidation and reduction depend critically on the reaction temperature. At temperatures under 450 K, the surface oxide coverage is practically frozen. In the temperature range of 500–550 K, the surface oxide coverage is dynamic, but formation and decomposition of the Pd oxides are rather slow processes. At higher temperatures and pressures, however, a much faster dynamic response may be expected.

3.5. Discussion of surface oxide coverage under reactions conditions

To analyze the dynamic oxidation and reduction behavior of the Pd particles in more detail, we now estimate the degree of surface oxidation under reaction conditions. For this purpose, we focus on the quasi-steady-state experiment at 500 K on the sample preoxidized at 550 K (see Figs. 5b–5d for experimental data).

As a first step, we need to consider that Pd surface oxides are always formed under O-rich conditions and decompose under CO-rich conditions at 500 K as shown experimentally earlier (see Section 3.4). Based on data from recent comprehensive MB studies on the formation of Pd oxides, we can assume that the rate of oxidation may be roughly approximated by a first-order kinetics [26,28]. Here it must be taken into account that the maximum Pd oxide coverage depends critically on the oxidation temperature. Therefore, we tentatively describe Pd oxidation rate as

$$\frac{\mathrm{d}\theta_{\mathrm{Oxide}}}{\mathrm{d}t} = k'_{\mathrm{Oxidation}}\theta_{\mathrm{O}}\left(1 - \frac{\theta_{\mathrm{Oxide}}}{\theta_{\mathrm{Oxide,max}}(T)}\right). \quad (1)$$

Here $\theta_{\mathrm{Oxide,max}}(T)$ denotes the maximum oxide coverage that can be obtained at a certain oxidation temperature (T), and $k_{\mathrm{oxidation}}$ denotes the effective rate constant of the Pd oxide formation. To evaluate the oxygen coverage under quasi-steady-state conditions, we assume that the oxygen coverage scales linearly with oxygen partial pressure in the O-rich regime until it finally becomes zero at the transition point,

$$\frac{\mathrm{d}\theta_{\mathrm{Oxide}}}{\mathrm{d}t} = k_{\mathrm{Oxidation}}\frac{(p_{\mathrm{O_2}}(t) - p_{\mathrm{O_2,Transition}})}{(p_{\mathrm{O_2,max}} - p_{\mathrm{O_2,Transition}})} \times \left(1 - \frac{\theta_{\mathrm{Oxide}}}{\theta_{\mathrm{Oxide,max}}(T)}\right). \quad (2)$$

For the Pd oxide decomposition, we follow a similar approach. As discussed elsewhere, CO oxidation involving Pd oxide species proceeds mainly via the slow decomposition of Pd oxide, which releases oxygen onto the metallic Pd surface, where it readily reacts with CO [26,28]. However, according to recent MB titration and IRAS experiments, the overall kinetics of CO oxidation involving Pd oxide species can be approximately described by first-order kinetics, provided that the degree of oxidation is not too high [28],

$$\frac{\mathrm{d}\theta_{\mathrm{Oxide}}}{\mathrm{d}t} = -k'_{\mathrm{Reduction}}\theta_{\mathrm{CO}}\theta_{\mathrm{Oxide}}. \quad (3)$$

Again, $k_{\mathrm{Reduction}}$ is an effective rate constant for Pd oxide decomposition. Similar to oxygen coverage, we further assume that CO coverage increases linearly with the CO partial pressure in the CO-rich regime, whereas it is negligibly small under O-rich conditions,

$$\frac{\mathrm{d}\theta_{\mathrm{Oxide}}}{\mathrm{d}t} = -k_{\mathrm{Reduction}}\frac{(p_{\mathrm{CO}}(t) - p_{\mathrm{CO,Transition}})}{(p_{\mathrm{CO,max}} - p_{\mathrm{CO,Transition}})}\theta_{\mathrm{Oxide}}. \quad (4)$$

To evaluate the Pd surface oxide coverage under reaction conditions using kinetic rate Eqs. (2) and (4), we have to define the boundary conditions. First, we estimate the upper limit for surface oxide formation at 500 K (reaction temperature) and 550 K (preoxidation temperature). Recent IRAS and MB titration experiments [28], as well as the data on deactivation of the model catalyst at low reaction temperatures due to preoxidation (Section 3.3), yields a maximum surface oxide coverage of approximately $\theta_{\mathrm{Oxide,max}} = \sim 0.35$ and ~ 0.55 at 500 and 550 K, respectively. Hence we assume the surface oxide coverage to be $\theta_{\mathrm{Oxide}} = 0.55$ after preoxidation in the beginning of the experiment. Next, the surface oxide coverage during the experiment is estimated as follows:

(1) *First run (increasing x_{CO}), O-rich conditions ($x_{\mathrm{CO}} < 0.6$).* The CO_2 formation rate scales linearly with the CO flux (see first run in Fig. 5b), indicating that the activity of the model catalyst remains constant. Therefore, we assume that the surface oxide coverage also remains constant at $\theta_{\mathrm{Oxide}} = 0.55$ up to $x_{\mathrm{CO}} < 0.6$ (see Fig. 6b). Considering that the upper limit for the surface oxide coverage at 500 K is significantly smaller than $\theta_{\mathrm{Oxide}} = 0.55$, this assumption appears reasonable.

(2) *First run (increasing x_{CO}) and second run (decreasing x_{CO}), CO-rich conditions ($x_{\mathrm{CO}} > 0.6$).* The surface oxide coverage under CO-rich conditions can be obtained by solving Eq. (4), describing the reduction of Pd oxide. In the next step, the effective rate constant $k_{\mathrm{Reduction}}$ of oxide decomposition must be estimated. Although the experimental data do not yield any explicit information about the oxide coverage, changes in the metallic Pd surface area are

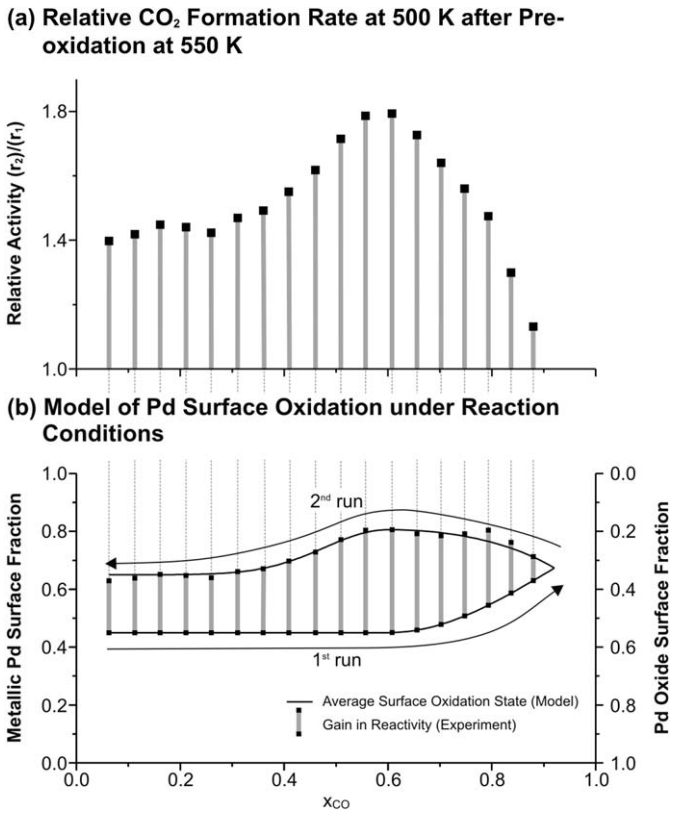

Fig. 6. Surface oxidation of the Pd/Fe_3O_4 catalyst under reaction condition at 500 K after preoxidation at 550 K: (a) relative CO oxidation activity during 2nd run (increasing O_2 flux, decreasing CO flux) relative to the 1st run (decreasing O_2 flux, increasing CO flux) as an indicator for changes of the metallic Pd surface area during the experiment; (b) estimated fractions of metallic Pd surface and Pd surface oxide on the particles during the CO oxidation.

indirectly reflected by the enhanced CO_2 formation rate during the second run normalized with respect to the first run (Fig. 6a). As discussed in the previous paragraph, the relative activity can be considered to be an indicator of the increase of metallic Pd surface area available for CO oxidation during the second run compared with the first run. For example, it follows that the metallic Pd surface at the transition point ($x_{CO} = 0.6$) in the second run is approximately ~1.8 times larger than in the first run, yielding $\theta_{Oxide} = 0.19$. Using this information, we can fit $k_{Reduction}$ to match the relative activity data ($k_{Reduction} = 8 \times 10^{-4}\ s^{-1}$). The result of this fit is shown in Fig. 6b (black curve). The gray bars indicate the gain in metallic Pd surface in the second run.

(3) *Second run (decreasing x_{CO}), O-rich conditions ($x_{CO} < 0.6$).* The oxide coverage during the second run under O-rich conditions can be obtained from Eq. (2). As boundary conditions, we use $\theta_{Oxide} = 0.19$ at the transitions point ($x_{CO} = 0.6$), which we have derived from solving Eq. (4), and the upper limit for the oxide formation at 500 K $\theta_{Oxide,max}(500\ K) = 0.35$ (see above). Similar to oxide decomposition, the effective rate constant for oxide formation $k_{Oxidation}$ is then fitted to match the relative activity data ($k_{Oxidation} = 6 \times 10^{-3}\ s^{-1}$).

The metallic Pd surface area and surface oxide coverage during the quasi-steady-state experiments are depicted in Fig. 6b. After preoxidation at 550 K, no further oxidation under O-rich conditions is observed because of the high surface oxide coverage obtained by preoxidation. Switching to CO-rich conditions, the metallic Pd surface fraction increases slowly due to partial reduction of surface oxides by CO. As a result, the CO oxidation activity is higher in the second run than in the first run. In the O-rich regime of the second run, a reoxidation of the Pd surface occurs that is connected to decreasing activity. Due to a kinetic hindrance of oxide formation at 500 K, however, the oxide coverage remains lower and the reaction rate higher during the second run than during the first run. It should be noted that the present model represents only a first estimate of the surface coverage; nonetheless, the model allows us to qualitatively understand the dynamic surface oxidation behavior on supported Pd catalyst surfaces independent of the composition of the reactant atmosphere.

4. Conclusion

In this contribution we have studied CO oxidation kinetics on metallic and partially oxidized Pd nanoparticles, combining fully automated MB and TR-IRAS experiments. Two temperature regimes for CO oxidation on partially oxidized Pd nanoparticles have been identified:

(i) *Low-temperature regime ($T < 450\ K$).* At low reaction temperatures, formation and decomposition of Pd surface oxides is kinetically hindered. As a result, metallic Pd particles remain metallic, independent of the reaction conditions, and no oxidation of the Pd particle surface is observed. Partial preoxidation of the Pd surface at higher temperatures leads to a permanent decrease in CO oxidation activity. The relative loss in activity is independent of the composition of the reactant environment, but depends on the degree of surface oxidation. We conclude that CO oxidation occurs mainly on metallic Pd surface areas, whereas the activity of Pd surface oxides is drastically lower. Even after extended exposure to a CO-rich environment ($>10^4$ s), no significant reduction of Pd surface oxides by CO is observed. It follows that the formation of surface oxides at higher temperatures leads to long-term deactivation of the catalyst surface at lower reaction temperatures.

(ii) *High-temperature regime ($T > 500\ K$).* At elevated reaction temperatures, Pd surface oxides can be dynamically formed and decomposed on the particles, depending on the composition of the reactant environment. Particle oxidation and reduction is directly coupled to the kinetic regimes of CO oxidation. Under O-rich conditions, the surface oxide coverage increases and asymptotically approaches a maximum value due to kinetic limitations of the oxidation process. The maximum surface oxide coverage rapidly increases at temperatures above 500 K. Under CO-rich conditions, the surface oxides decompose, and the catalyst activity increases. As a result, the surface oxidation state and the

activity of the Pd particles dynamically respond to the reactive environment and may drastically change over a very narrow range of stoichiometric conditions.

Acknowledgments

This work was funded by the Deutsche Forschungsgemeinschaft (SPP 1091) and the Fonds der Chemischen Industrie. The authors are particularly grateful to D.E. Starr and Sh.K. Shaikhutdinov for providing STM images.

References

[1] G. Ertl, H. Knoezinger, J. Weitkamp (Eds.), Handbook of Heterogeneous Catalysis, VCH, Weinheim, 1997.
[2] J.M. Thomas, W.J. Thomas, Principle and Practice of Heterogeneous Catalysis, VCH, Weinheim, 1997.
[3] H. Conrad, G. Ertl, J. Küppers, E.E. Latta, Surf. Sci. 65 (1977) 245.
[4] R. Imbihl, J.E. Demuth, Surf. Sci. 173 (1986) 395.
[5] S.-L. Chang, P.A. Thiel, J. Chem. Phys. 88 (1988) 2071.
[6] X. Guo, A. Hoffman, J.T. Yates Jr., J. Chem. Phys. 90 (1989) 5787.
[7] V.A. Bondzie, P. Kleban, D.J. Dwyer, Surf. Sci. 347 (1996) 319.
[8] E.H. Voogt, A.J.M. Mens, O.L.J. Gijzeman, J.W. Geas, Surf. Sci. 373 (1997) 210.
[9] F.P. Leisenberger, G. Koller, M. Sock, S. Surnev, M.G. Ramsey, F.P. Netzer, B. Klötzer, K. Hayek, Surf. Sci. 445 (2000) 380.
[10] V.A. Bondzie, P.H. Kleban, D.J. Dwyer, Surf. Sci. 465 (2000) 266.
[11] G. Zheng, E.I. Altman, Surf. Sci. 462 (2000) 151.
[12] G. Zheng, E.I. Altman, Surf. Sci. 504 (2002) 253.
[13] E. Lundgren, G. Kresse, C. Klein, M. Borg, J.N. Andersen, M. De Santis, Y. Gauthier, C. Konvicka, M. Schmid, P. Varga, Phys. Rev. Lett. 88 (2002) 246103.
[14] M. Todorova, E. Lundgren, V. Blum, A. Mikkelsen, S. Gray, J. Gustafson, M. Borg, J. Rogal, K. Reuter, J.N. Andersen, M. Scheffler, Surf. Sci. 541 (2003) 101.
[15] E. Lundgren, J. Gustafson, A. Mikkelsen, J.N. Andersen, A. Stierle, H. Dosch, M. Todorova, J. Rogal, K. Reuter, M. Scheffler, Phys. Rev. Lett. 92 (2004) 046101.
[16] M. Todorova, K. Reuter, M. Scheffler, Phys. Rev. B 71 (2005) 195403.
[17] A. Stierle, N. Kasper, H. Dosch, E. Lundgren, J. Gustafson, A. Mikkelsen, J.N. Andersen, J. Chem. Phys. 122 (2005) 44706.
[18] H. Over, Y.D. Kim, A.P. Seitsonen, S. Wendt, E. Lundgren, M. Schmid, P. Varga, A. Morgante, G. Ertl, Science 287 (2000) 1474.
[19] G. Zheng, E.I. Altman, J. Phys. Chem. B 106 (2002) 1048.
[20] B.L.M. Hendriksen, S.C. Bobaru, J.W.M. Frenken, Surf. Sci. 552 (2004) 229.
[21] C.R. Henry, Surf. Sci. Rep. 31 (1998) 231.
[22] V.P. Zhdanov, B. Kasemo, Surf. Sci. Rep. 39 (2000) 25.
[23] T.P.St. Clair, D.W. Goodman, Top. Catal. 13 (2000) 5.
[24] H.-J. Freund, M. Bäumer, J. Libuda, T. Risse, G. Rupprechter, S. Shaikhutdinov, J. Catal. 216 (2003) 223.
[25] J. Libuda, H.-J. Freund, Surf. Sci. Rep. 57 (2005) 157.
[26] T. Schalow, M. Laurin, B. Brandt, S. Schauermann, S. Guimond, H. Kuhlenbeck, D.E. Starr, S.K. Shaikhutdinov, J. Libuda, H.-J. Freund, Angew. Chem. Int. Ed. 44 (2005) 7601.
[27] T. Schalow, B. Brandt, D.E. Starr, M. Laurin, S. Schauermann, S.K. Shaikhutdinov, J. Libuda, H.-J. Freund, Catal. Lett. 107 (2006) 189.
[28] T. Schalow, B. Brandt, M. Laurin, S. Schauermann, S. Guimond, H. Kuhlenbeck, J. Libuda, H.-J. Freund, Surf. Sci. 600 (2006) 2528.
[29] J. Libuda, I. Meusel, J. Hartmann, H.-J. Freund, Rev. Sci. Instrum. 71 (2000) 4395.
[30] W. Weiss, W. Ranke, Prog. Surf. Sci. 70 (2002) 1.
[31] C. Lemire, R. Meyer, V. Henrich, S.K. Shaikhutdinov, H.-J. Freund, Surf. Sci. 572 (2004) 103.
[32] R. Meyer, S.K. Shaikhutdinov, H.-J. Freund, Z. Phys. Chem. 218 (2004) 905.
[33] L. Piccolo, C. Becker, C.R. Henry, Appl. Surf. Sci. 164 (2000) 156.
[34] J. Libuda, I. Meusel, J. Hoffmann, J. Hartmann, L. Piccolo, C.R. Henry, H.-J. Freund, J. Chem. Phys. 114 (2001) 4669.
[35] P. Hollins, Surf. Sci. Rep. 16 (1992) 51.
[36] I. Meusel, J. Hoffmann, J. Hartmann, J. Libuda, H.-J. Freund, J. Phys. Chem. B 105 (2001) 3567.
[37] J. Hoffmann, I. Meusel, J. Hartmann, J. Libuda, H.-J. Freund, J. Catal. 204 (2001) 378.
[38] T. Engel, G. Ertl, in: D.A. King, D.P. Woodruff (Eds.), The Chemical Physics of Solid Surfaces and Heterogeneous Catalysis, Elsevier, Amsterdam, 1982, p. 73.
[39] T. Schalow, B. Brandt, D.E. Starr, M. Laurin, S.K. Shaikhutdinov, S. Schauermann, J. Libuda, H.-J. Freund, Angew. Chem. Int. Ed. 45 (2006) 3693.